Journal of Applied Fluid Mechanics, Vol. 13, No. 2, pp. 737-751, 2020.
Available online at www.jafmonline.net, ISSN 1735-3572, EISSN 1735-3645.
DOI: 10.29252/jafm.13.02.30310

Investigation of Breakup and Coalescence Models for Churn-Turbulent Gas-Liquid Bubble Columns

T. Matiazzo, R. K. Decker, J. C. S. C. Bastos, M. K. Silva and H. F. Meier†

University of Blumenau, Blumenau, Santa Catarina, 89030-000, Brazil

†*Corresponding Author Email: meier@furb.br*

(Received March 28, 2019; accepted July 20, 2019)

ABSTRACT

Three-dimensional Eulerian-Eulerian transient simulations were conducted to represent the gas-liquid flow of a heterogeneous bubble column. Different drag closures, breakup and coalescence models were evaluated in order to verify their influence on the model prediction. Numerical simulations were compared to experimental data, with industrial conditions of gas superficial velocities: 20*cm/s* and 40*cm/s*, in order to select the most suitable models to describe the bubble' dynamics in the heterogeneous flow. The standard $k-\varepsilon$ model for both phases was set for turbulence. 12 combinations of breakup and coalescence models were compared and analyzed. In the case of coalescence, Models of Prince and Blanch, and Luo presented similar behavior and good agreement with experimental data, while for breakup, a breakage forming three daughter bubbles appeared to be the best choice. Simulations presented relative errors around 7.7% and 14.0%, for 20*cm/s* and 40*cm/s* respectively, for the gas axial velocity, and around 14% and 21.9%, for gas holdup. For drag force, density and viscosity were accounted by an average of the phases, which resulted in an improvement about 7% on model validation

Keywords: CFD simulation; Population balance; Breakup; Coalescence; Churn turbulent flow.

NOMENCLATURE

B_b	breakup birth rate
B_c	coalescence birth rate
b	breakup frequency
C_1	breakage kernel constant
C_2	breakage kernel constant
C_3	breakage kernel constant
C_b	breakup death rate
C_c	coalescence death rate
C_D	drag coefficient
$C_{1\varepsilon}$, $C_{2\varepsilon}$, $C_{3\varepsilon}$	turbulence model constant
C_μ	turbulence viscosity constant
$C_{p,q}$	Standard $k-\varepsilon$ constant, 2.0
$C_{q,p}$	Standard $k-\varepsilon$ constant $2\left(\frac{\eta_{p,q}}{1+\eta_{p,q}}\right)$
C	coalescence rate
c	continuous phase index
d	diameter
d	dispersed phase index
f_v	breakup volume fraction
G	turbulent production term
$\vec{g}$	gravity acceleration vector
h	mean square velocity
h_0	initial film thickness
h_f	critical film thickness
I	unit vector
i	particle size index
j	particle size index
$K_{p,q}$	interphase momentum exchange coefficient
k	Turbulent kinetic energy
k	generic phase index
$M_{c,d}$	momentum exchange
n	number density
P	coalescence efficiency
p	pressure
p_c	number of daughters produced in breakage
p_i	p_c in the *ith* term of generalized form
q_i	extended Hill-Ng daughter distribution parameter
p	secondary phase index
p	primary phase index
r	bubble radius
r_i	extended Hill-Ng parameter
Re	Reynolds number
t	time
U	Phase-weight velocity
$\vec{u}$	velocity vector
V_{0m}	maximum relative velocity magnitude
v	volume
v'	daughter particle volume

We	Weber number
w	collision frequency
w_i	weight of *ith* term
z	self-similar daughter size
α	void fraction
β	daughter bubble size distribution
$\dot{\gamma}$	shear rate
μ	viscosity
ρ	density
σ	surface tension
$\sigma_{u_i}^2$	variance for Das (2015) coalescence closure
$\sigma_{u_j}^2$	variance for Das (2015) coalescence closure
σ_k	turbulent Prandtl number for k
σ_ε	turbulent Prandtl number for ε
ε	turbulent kinetic energy dissipation rate
ς_T	capture efficiency prefactor
$\vec{\tau}$	strain stress
ξ	eddy size divided by parent bubble size

1. INTRODUCTION

A bubble column consists of a cylindrical vessel filled with liquid or a liquid-solid suspension, with a gas distributor at the bottom. The main advantage of this equipment is the high mass and heat transfer rates, with low operational and maintenance costs, due to the lack of moving parts and compactness allied to the fact that the contact between the phases occurs without the addition of mechanical stirring (Kantarci *et al.*, 2005; Rollbusch *et al.*, 2015 and Leonard *et al.*, 2015).

The versatility of bubble columns as either reactors or multiphase contactors has led to their extensive use at several types of plants in the chemical, biochemical and petrochemical industries. In bubble column reactors, three important mechanisms influence both the design and scale-up of the column: the heat and mass transfer, mixing characteristics and chemical kinetics of the reacting system (Kantarci *et al.*, 2005). The fluid dynamics behavior of bubble columns is not yet fully understood and is difficult to predict. It is dependent on bubble rise, bubble-bubble and bubble-liquid interactions, bubble size and size distribution and gas hold-up (Leonard *et al.*, 2015). Bubble columns can operate with a homogeneous or heterogeneous flow regime depending on the superficial gas velocity, column diameter, physical properties of the components, and type of gas distribution, pressure and temperature (Rollbusch *et al.*, 2015). The flow regime can be categorized into four main groups: perfect bubbly flow, imperfect bubbly flow, churn-turbulent and slug flow (Fig. 1). At high superficial gas velocities, the churn-turbulent flow is observed and this is the regime most commonly present at industrial applications. In this regime, the breakup and coalescence phenomena gain importance, since the flow is characterized by the coexistence of small and large bubbles (i.e., a wide bubble size distribution) as a result of bubble coalescence and breakup. The lack of homogeneity of the gas distribution causes recirculation, where liquid rises at the center of the vessel and flows downwards near the walls (Leonard *et al.*, 2015 and Sathe *et al.*, 2013).

CFD studies on this regime have become come more numerous in recent years (Wang and Wang, 2007; Silva *et al.*, 2012; Xu *et al.*, 2013; Liu and Hinrichsen, 2014; Silva *et al.*, 2014; Guan *et al.*, 2015 and Sharaf *et al.*, 2016). Researches have been investigating different approaches to the turbulence closure, such as direct numerical simulation, large eddy simulation, Reynolds stress, k-ε, among others (Ma *et al.*, 2015; Montoya *et al.* 2016; Ma *et al.*, 2016; Tryggvason *et al.*, 2016; Joshi *et al.*, 2017 and Tryggvason *et al.*, 2018).

The complex direct numerical simulation approach associated with a statistical method has also been used to optimize interfacial momentum closures (Liu *et al.*, 2017 and Liu and Dinh, 2019).

Although, several models of breakup and coalescence have been proposed in the literature, for instance, some described by Liao and Lucas (2009), Liao and Lucas (2010) and Sajjadi *et al.* (2013), few authors have carried out an evaluation and comparison between the approaches available in the literature.

Chen *et al.* (2005) conducted numerical simulations for a wide range of superficial velocities in columns with distinct diameters, covering the homogeneous, transitional and heterogeneous flow regimes. The authors conducted bi-dimensional simulations and found good agreement with experimental data when the breakup rate was increased by a factor of ten, independently of the breakup and coalescence approaches employed. The research also highlighted the importance of three-dimensional simulations to obtain good agreement for the gas holdup as well as the crucial use of a population balance to represent the heterogeneous flow in Euler-Euler modeling.

More recently, Deju *et al.* (2015) conducted numerical experiments varying the combination of breakup and coalescence models, with a total of seven distinct combinations. The authors found good agreement between simulations and experimental data with regards to the interfacial area concentration and gas velocity profile predictions. However, the authors noted that the limited amount of experimental data available and the high number of assumptions in breakup and coalescence models do not permit the identification of the most appropriate combination.

In this context, in this study, 12 combinations of breakup and coalescence models were evaluated, and numerical simulations were compared with experimental data of Manjrekar and Dudukovic (2015) in order to validate the model predictions.

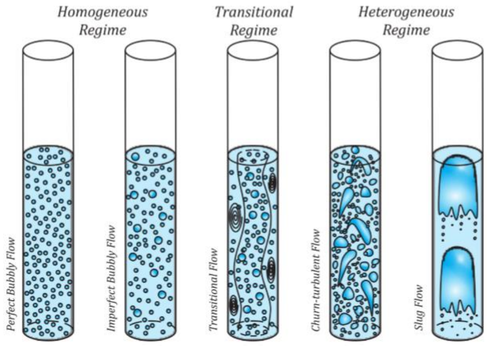

Fig. 1. Diagrams showing different flows regimes.

2. MATHEMATICAL MODELING

In this study, the heterogeneous flow in bubble columns was modeled according to a Euler-Euler approach associated with a homogeneous population balance. Table 1 provides details of the conservation equations of mass and momentum, along with turbulence closure and population balance equations.

2.1 Drag Closure

The resistance to bubble motion imposed by the surrounding liquid is referred to as the drag force and is expressed in Eq. (4) (Rzehak and Krepper, 2015). According to several authors (Wörner, 2003; Sannáes and Schanke, 2004; Chen *et al.* 2005; Silva *et al.*, 2012), drag is the dominant interfacial force, and with the appropriated model, the contribution of lift, wall lubrication, virtual mass and turbulent dispersion can be neglected. This dominance is more accentuated in the heterogeneous regime.

Based on that, three approaches to evaluate the drag coefficient were tested: (i) the model of Schiller and Naumann (1935); (ii) a modified version of (i), called the Symmetric model; and (iii) the model proposed by Zhang and Vanderheyden (2002).

Schiller and Naumann (1935) and Symmetric models difference lies in the calculation of the density and viscosity. In contrast to the original model of Schiller and Naumann (1935), the Symmetric model uses volume-averaged density and viscosity, as shown in Table 2.

2.2 Turbulence

The liquid phase turbulence has two influential components at multiphase flows. Besides the expected turbulence of any liquid flow, the gas-liquid interaction, in the form of bubble motion, also creates turbulence (Wang and Yao, 2016). Bubble's movement in the liquid phase induces velocity fluctuations which can be immediately dissipated by viscosity, or it can generate movement in bigger scales (Lelouvetel *et al.* 2014).

According to Joshi *et al.* (2017), when the flow is homogeneous, the transfer of energy from gas to liquid is negligible duo to the lack of hindrance to the bubble motion. However, the same cannot be stated for heterogeneous flows, therefore turbulence induced by bubble motion gains significance in heterogeneous bubble columns.

Frequently, turbulence is applied only for the continuous phase, and the contribution for it made by the bubble passage is accounted modeling bubble induced turbulence (Chen *et al.* 2005; Joshi *et al.*, 2017; Silva *et al.*, 2012; Silva *et al.*, 2014 and Soccol *et al.*, 2015).

In this case, due to the high gas superficial velocity, turbulence was applied for both phases, using the standard k-ε model, which is based on Boussinesq hypothesis, assuming Reynolds stress tensors proportional to mean velocity gradients and isotropy.

The standard k-ε approach proposed by Launder and Spalding (1972) has four empirical constants and is known to overpredict the gas void fraction close to the wall (Yamoah *et al.*, 2015; Deju *et al.*, 2013). However, this approach has been proven to be efficient with a lower computational cost than other turbulence modeling (Chen *et al.* 2005; Silva *et al.*, 2012 and Soccol *et al.*, 2015).

For evaluating its influence in the flow, bubble induced turbulence (BIT) was applied by Sato and Sekoguchi (1975) model, which consists in the addition of a second term on the effective viscosity equation, as expressed in Eq. (13) (Table 1).

2.3 Population Balance

Population balance equations have been applied to several chemical engineering problems since Hulburt and Katz (1964) first used this approach for particulate systems. The equation is a statistical way to describe the dispersed phase in a multi-phase flow. A generic equation for the population balance applied to bubble columns is represented in Eq. (8) (Table 1), neglecting mass transfer as well as growth and nucleation terms. The terms on the right-hand side of Eq. (8) correspond to the source terms of coalescence and breakage. Equations (9) and (10) represent the birth and death for the coalescence phenomena while Eqs. (11) and (12) are the birth and death for breakage.

2.4 Breakage kernels

In general, breakage is a consequence of the fluid dynamics characteristics of the continuous phase as well as the interfacial interactions. However, it is not yet fully understood (Jakobsen *et al.*, 2005) and several models have been proposed in literature, based on four mechanisms: turbulent fluctuation and collision (Liao and Lucas, 2009,Wang, 2011, Sajjadi *et al.*, 2013); viscous shear stress (Liao and Lucas, 2009; Liao, 2014; the shearing-off process; and interfacial instability. In this study, three breakup models were analysed, with the breakup closures given in Table 3.

Luo and Svendsen (1996): This model applies isotropic turbulence and probability, assuming binary breakage, and is one of the models most commonly used in recent literature. It is based on turbulence fluctuations and collision mechanism, along with a comparison of the turbulent kinetic energy of the hitting eddy with a critical value.

Table 1 A summary of the governing and constitutive equations

Governing equations		
Mass conservation:	$\frac{\partial}{\partial t}(\rho_k \alpha_k) + \frac{\partial}{\partial t}(\rho_k \alpha_k \mathbf{u}_k) = 0$	(1)
Momentum conservation:	$\frac{\partial}{\partial t}(\rho_k \alpha_k \mathbf{u}_k) + \frac{\partial}{\partial t}(\rho_k \alpha_k \mathbf{u}_k \mathbf{u}_k) = -\alpha_k \nabla p - \nabla.(\alpha_k \tau_k) + \alpha_k \rho_k \mathbf{g} + \mathbf{M}_{cd}^{D}$	(2)
Constitutive equations		
Strain stress:	$\tau_k = \mu_k \left(\nabla \mathbf{u}_k + (\nabla \mathbf{u}_k)^T - \frac{2}{3}(\nabla.\mathbf{u}_k)\mathbf{I} \right) + \alpha_k$	(3)
Drag:	$\mathbf{M}_{cd}^{D} = \frac{3}{4} C_D \rho_c \frac{\alpha_d}{d_d}(u_d - u_c)\lvert u_d - u_c \rvert$	(4)
Turbulence equations k-ε for each phase		
Turbulent Viscosity:	$\mu_{t,q} = C_{\mu} \rho_q \frac{k_q^2}{\varepsilon_q}$	(5)
Transport equation for k:		
$\frac{\partial}{\partial t}(\alpha_q \rho_q k_q) + \nabla.(\alpha_q \rho_q \mathbf{U}_q k_q) = \nabla.\left[\alpha_q \left(\mu_q + \frac{\mu_{t,q}}{\sigma_k}\right)\nabla k_q\right] + (\alpha_q G_{k,q} - \alpha_q \rho_q \varepsilon_q) + \sum_{p=1}^{n} K_{p,q}(C_{p,q} k_p - C_{q,p} k_q) - \sum_{p=1}^{n} K_{p,q}(\mathbf{U}_p - \mathbf{U}_q)\frac{\mu_{t,p}}{\alpha_p \sigma_p}\nabla \alpha_p + \sum_{p=1}^{n} K_{p,q}(\mathbf{U}_p - \mathbf{U}_q)\frac{\mu_{t,q}}{\alpha_q \sigma_q}\nabla \alpha_q$		(6)
Transport equation for ε:		
$\frac{\partial}{\partial t}(\alpha_q \rho_q \varepsilon_q) + \nabla.(\alpha_q \rho_q \mathbf{U}_q \varepsilon_q) = \nabla.\left[\alpha_q \left(\mu_q + \frac{\mu_{t,q}}{\sigma_\varepsilon}\right)\nabla \varepsilon_q\right] + C_{1\varepsilon}\frac{\varepsilon_q}{k_q}\alpha_q G_{k,q} - C_{2\varepsilon}\frac{\varepsilon_q}{k_q}\alpha_q \rho_q \varepsilon_q + C_{3\varepsilon}\frac{\varepsilon_q}{k_q}K_{p,q}(C_{p,q} k_p - C_{q,p} k_q) - C_{3\varepsilon}\frac{\varepsilon_q}{k_q}K_{p,q}(\mathbf{U}_p - \mathbf{U}_q)\frac{\mu_{t,p}}{\alpha_p \sigma_p}\nabla \alpha_p + C_{3\varepsilon}\frac{\varepsilon_q}{k_q}K_{p,q}(\mathbf{U}_p - \mathbf{U}_q)\frac{\mu_{t,q}}{\alpha_q \sigma_q}\nabla \alpha_q$		(7)
$C_{\mu} = 0.09;\ C_{1\varepsilon} = 1.44;\ C_{2\varepsilon} = 1.92;\ C_{3\varepsilon} = 1.2;\ \sigma_k = 1.0;\ \sigma_\varepsilon = 1.3$		
Population balance equations		
	$\frac{\partial n(v,t)}{\partial t} + \nabla(\mathbf{u}_d n(v,t)) = B_c + D_c + B_b + D_b$	(8)
Coalescence birth rate:	$B_c = \frac{1}{2}\int_0^{v} c(v - v', v') n(v - v', v') n(v', t) dv'$	(9)
Coalescence death rate:	$c(v, v') n(v', t) dv'$	(10)
Breakup birth rate:	$B_b = \int_0^{\infty} pb(v')\beta(v, v') n(v', t) dv'$	(11)
Breakup death rate:	$D_b = -b(v) n(v,t)$	(12)
Bubble Induced Turbulence		
Sato and Sekoguchi (1975):	$\mu_{t,q} = C_{\mu} \rho_q \frac{k_q^2}{\varepsilon_q} + C_{\mu,p} \rho_p \alpha_p d_p \lvert \mathbf{U}_p - \mathbf{U}_q \rvert$	(13)

Lehr *et al.* (2002) based their work on the Luo and Svendsen (1996) kernel with regard to the probability that collisions will result in breakage. Therefore, both models assume isotropic turbulence, based on the considerations of Hinze (1959), besides expressing a collision frequency analogous to kinetic theory.

Laakkonen *et al.* (2006): These authors carried out a parametric study of the model presented by Alopaeus *et al.* (2002), which is a modified version of that initially proposed by Narsimhan *et al.* (1979). A stochastic model computes the breakage frequency, assuming that the arrival of eddies with different length scales can be described by a Poisson process. Again, turbulence fluctuation and collision are considered to be the mechanism responsible for breakup, considering that if the velocity fluctuation

Table 2 Drag Coefficient

Schiller and Naumann (1935): $C_D = \begin{cases} \dfrac{24(1+0.15Re^{0.687})}{Re} & \text{if } Re < 1000 \\ 0.44 & \text{if } Re > 1000 \end{cases}$		(14)
Zhang and Vanderheyden (2002): $C_D = 0.44 + \dfrac{24}{Re} + \dfrac{6}{1+\sqrt{Re}}$		(15)
Symmetric	*Equation* (14)	
* for the Symmetric Model, the density and viscosity are averaged between phases (ρ_{pq}, μ_{pq})		

Where $Re = \dfrac{\rho_q d_p \left|\mathbf{u}_p - \mathbf{u}_q\right|}{\mu_q}$

Table 3 Breakup closures

Luo and Svendsen (1996):

Breakup frequency:
$$b(d) = \int_0^{0.5} b(f_v|d)\,df_v \quad (16)$$

$$b(f_v|d) = 0.923(1-\alpha_g)\left(\frac{\varepsilon}{d^2}\right)^{1/3}\int_{\xi_{min}}^{1}\frac{(1+\xi)^2}{\xi^{11/3}}exp\left\{-\frac{12\left[f_v^{2/3}+(1-f_v)^{2/3}-1\right]\sigma}{\rho_d\,\varepsilon^{2/3}d^{5/3}\xi^{11/3}}\right\} \quad (17)$$

PDF:
$$\beta(f_v,d) = \frac{b(f_v|d)}{\int_0^{0.5} b(f_v|d)\,df_v} \quad (18)$$

Lehr *et al.* (2002):

Breakup frequency:
$$b(d) = 0.5\frac{d_i^{5/3}\varepsilon^{19/15}\rho_c^{7/5}}{\sigma^{7/5}}exp\left(-\frac{\sqrt{2}\sigma^{9/5}}{d_i^3\rho_c}\right) \quad (19)$$

PDF:
$$\beta(f_v,d) = \frac{1}{\sqrt{\pi}f_v}\frac{exp\left\{-\frac{9}{4}\left[ln\left(\frac{2^{2/5}d_i\,p_c^{3/5}\varepsilon^{2/5}}{\sigma^{3/5}}\right)\right]^2\right\}}{\left\{1+erf\left[\frac{3}{2}ln\left(\frac{2^{1/15}d_i\rho_c^{3/5}\varepsilon^{2/5}}{\sigma^{3/5}}\right)\right]\right\}} \quad (20)$$

Laakkonen *et al.* (2006):

Breakup frequency:
$$b(d) = C_1\varepsilon^{1/3}erfc\left(\sqrt{C_2\frac{\sigma}{\rho_c\varepsilon^{2/3}d^{5/3}} + C_3\frac{\mu_d}{\sqrt{\rho_c\rho_d}\,\varepsilon^{2/3}d^{5/3}}}\right) \quad (21)$$

Laakkonen *et al.* (2006) PDF:
$$\beta(\nu,\nu') = \frac{30}{\nu'}\left(\frac{\nu}{\nu'}\right)^2\left(1-\frac{\nu}{\nu'}\right)^2 \quad (22)$$

Generalized PDF:
$$p\beta(\nu,\nu') = \frac{1}{\nu'}\sum_i w_i\,p_i\frac{z^{q_i-1}(1-z)^{r_i-1}}{\beta(q_1,r_i)} \quad (23)$$

Table 4 Coalescence closures

Prince and Blanch (1990):		
Coalescence closure:	$c(d_i,d_j)=w(d_i,d_j)P(d_i,d_j)$	(24)
Coalescence efficiency:	$w(d_i,d_j)=0.89\pi(d_i,d_j)^2\varepsilon^{1/3}(d_i^{2/3},d_j^{2/3})^{\frac{1}{2}}$	(25)
Coalescence efficiency:	$P(d_i,d_j)=\exp\left[-\dfrac{\left(\dfrac{r_{ij}^3\rho_c}{16\sigma}\right)^{1/2}\varepsilon^{1/2}ln\dfrac{h_0}{h_f}}{r_{ij}^{2/3}}\right]$	(26)
Luo (1993):		
Coalescence closure:	$c(d_i,d_j)=w(d_i,d_j)P(d_i,d_j)$	(27)
Collision frequency:	$w(d_i,d_j)=\dfrac{\pi}{4}\sqrt{2}(d_i,d_j)^2\varepsilon^{1/3}(d_i^{2/3},d_j^{2/3})^{\frac{1}{2}}$	(28)
Coalescence efficiency	$P(d_i,d_j)=exp\left\{-c_1\dfrac{\left[0.75\left[1+(d_i/d_j)^2\right]+\left[1+(d_i/d_j)^3\right]\right]^{1/2}}{\left(\dfrac{\rho_g}{\rho_d}+0.5\right)^{1/2}\left[1+(d_i/d_j)^3\right]}We_{ij}^{1/2}\right\}$	(29)
Das (2015):		
Coalescence closure:	$c(d_i,d_j)=\sqrt{8\pi}r_{ij}^2\left(\sigma_{u_i}^2+\sigma_{u_j}^2\right)\left[1-exp\left(-\dfrac{1}{2}\dfrac{V_{0m}^2}{\left(\sigma_{u_i}^2+\sigma_{u_j}^2\right)}\right)\right]$	(30)

around the particle surface is greater than a critical value breakage occurs Liao and Lucas (2009). In contrast to the Luo and Svendsen (1996) and Lehr *et al.* (2002) models, where the size distribution of the daughter particles is derived directly from the breakup rate expression, the Laakkonen *et al.* (2006) model requires an additional equation for the size distribution of the daughter particles. In this paper, two approaches were taken into consideration, one proposed by Laakkonen *et al.* (2006) and the other known as generalized approach. The former approach has several adjustable parameters and the main advantage is a low computational requirement, due to its simplicity. The latter allows, besides others parameters, the selection of the number of daughter particles that each breakup event will generate, differently from the other models that assume a binary breakage. According to the experiments of Risso and Fabre (1998), around 48%of breakage events produce two daughter particles and approximately 37% produce from 3 to 7 daughters. Therefore, the generalized distribution, initially proposed by Diemer and Olson (2002), was tested selecting 3 as the number of daughters generated at each breakup event.

2.5 Coalescence kernels

According to Chesters (1991) and Liao and Lucas (2010) coalescence is a more complex mechanism than breakup, since it is dependent not only on interactions between the particle and its surroundings, but also on interactions between particles themselves and of the forces that bring them together. It is modeled as the product of the collision frequency and coalescence efficiency. The literature identifies five different mechanisms for collision: turbulence-induced collision; viscous shear-induced collision; buoyancy-induced collision; wake-entrainment; and capture in turbulent eddies. Although all the five have a cumulative effect, most of the models assume one predominant mechanism as a simplification. Three different coalescence closures were analysed in this study and they are listed in Table 4.

Not every collision results in coalescence, therefore the efficiency term accounts for the probability of this event. Three criteria for coalescence efficiency are proposed in the literature:

- Film drainage theory (Shinnar and Church, 1960): is the most commonly used criteria, it is considered that after collision a liquid film is formed between the particles. The thickness of this film decreases with time; therefore, if the contact time is long enough the film reaches a critical minimal thickness leading to its rupture;

- Energetic theory (Howarth, 1964): considers that the occurrence of coalescence is determined by the intensity of the collision impact.
- Critical velocity: it is predicted that coalescence will occur if the relative velocity of the approach is greater than a critical value (Liao and Lucas, 2010 and Sajjadi *et al.*, 2013).

Prince and Blanch (1990): The modeling applied in this paper considers only turbulence-induced collision as a mechanism and for the collision probability the film drainage theory is considered.

Luo (1993): The mechanism is the same as that taken into account by Prince and Blanch (1990). However, different constants are used for multiplying the collision frequency term and a distinct approach is applied to the drainage time constraint.

Das (2015): This model introduces a new mathematical approach to the issue of coalescence. In contrast to most previously published models, coalescence is formulated as a single term that accounts for collision frequency and coalescence efficiency.

3. COMPUTATIONAL METHODOLOGY

A commercial CFD code Fluent 14 from ANSYS, which employs the finite volume method, was used to solve the transport equations. The phase-coupled SIMPLE was applied for pressure velocity coupling, and the class method for the population balance equations.

A hexahedral mesh was created using the software ANSYS ICEMCFD 14 to describe the facility used by Manjrekar and Dudukovic (2015), a plexiglass column with a height of 2*m* and a diameter of 20.32*cm*, operating with air and water. The experiments were carried out for two distinct superficial air velocities (20 and 40*cm/s*), with data being collected using 4-point optical probe (Xue *et al.*, 2008) at an approximate height of 75*cm*.

The chosen of a 196,010 control volumes mesh (Fig. 2) was based on a grid convergence index method proposed by Celik *et al.* (2008); it estimates the mesh refinement error based on the extrapolation theory of Richardson, using three different mesh sizes. For this case, three meshes were built, with refinement ratio of 1.3. Gas holdup and axial velocity were evaluated, and for both, the difference between the results of the most refined and the mesh used were about 4%. For the boundary conditions, at the entrance, velocities were specified for both phases; at the exit, gas phase pressure was defined as atmospheric, and no-slip were adopted for both phases at the wall. As initial condition liquid height was set to 1.2*m* for a gas superficial velocity of 20*cm/s* and at 0.9*m* for a gas superficial velocity of 40*cm/s*.

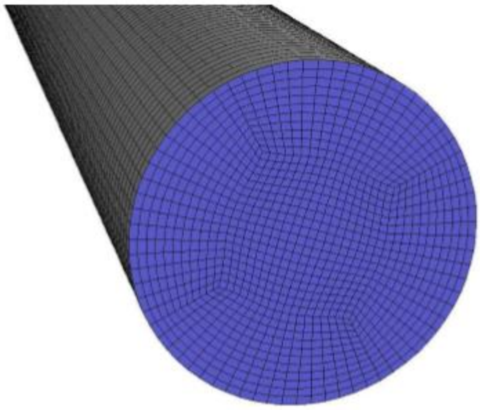

Fig. 2. Numerical mesh.

To optimize computational time, time step varied from 10^{-4} to 10^{-2}. Numerical results were carried out with an accuracy of RMS residuals less than 10^{-4}. Simulations were performed for 120s and the first 20*s* were used to achieve a quasi-stationary state; therefore, this period was not included in the calculation of the time-averaged variables.

To evaluate the influence of the model considerations, the effect of drag models, breakup and coalescence closures were investigated in order to provide a consistent mathematical approach for the heterogeneous flow regime in bubble columns. For the solution of population balance equations, the class method demands a bubble class size as initial condition, the bin number represents each size. It was selected a total of 9 bins, sized according to experimental data. To evaluate the influence of the drag model, three drag correlations were compared: the Schiller and Naumann (1935) model, a modified version of it, called Symmetric model, and the Zhang and Vanderheyden (2002) model. At this point the breakup of Luo and Svendsen (1996) and the coalescence kernel of Luo (1993) were employed.

After performing the drag model tests, different breakup and coalescence closures were analysed resulting in 24 simulations. Numerical simulations combining the four breakage closures (Luo and Svendsen, 1996; Lehr *et al.* (2002); Laakkonen *et al.* (2006) and Laakkonen *et al.* (2006) with Generalized PDF distribution) and the three coalescence closures (Prince and Blanch, 1990; Luo, 1993 and Das, 2015) were conducted for two superficial velocities, 20 and 40*cm/s*, as shown in Table 5. The others simulations settings are listed in Table 6.

4. RESULTS AND DISCUSSION

Heterogeneous bubbly flows are extremely difficult to predict, due to the complex phase interaction and the way in which bubbles break and coalesce during the process. Although several studies on bubbly flows are available in the literature, the effects of different drag closures combining with distinct breakup and coalescence models, and a experimental data comparison, do not seem to have been previously investigated in detail. All the numerical

Table 5 Summary of breakage and coalescence closures used in each numerical case

Case	Gas Superficial velocity	Breakup Closure	Coalescence Closure
Case05-9-20	20 cm/s	Luo and Svendsen (1996)	Prince and Blanch (1990)
Case06-9-20	20 cm/s	Lehr *et al.* (2002)	Prince and Blanch (1990)
Case07-9-20	20 cm/s	Laakkonen *et al.* (2006)	Prince and Blanch (1990)
Case08-9-20	20 cm/s	Laakkonen *et al.* (2006) + Generalized PDF	Prince and Blanch (1990)
Case09-9-20	20 cm/s	Luo and Svendsen (1996)	Luo (1993)
Case10-9-20	20 cm/s	Lehr *et al.* (2002)	Luo (1993)
Case11-9-20	20 cm/s	Laakkonen *et al.* (2006)	Luo (1993)
Case12-9-20	20 cm/s	Laakkonen *et al.* (2006) + Generalized PDF	Luo (1993)
Case13-9-20	20 cm/s	Luo and Svendsen (1996)	Das (2015)
Case14-9-20	20 cm/s	Lehr *et al.* (2002)	Das (2015)
Case15-9-20	20 cm/s	Laakkonen *et al.* (2006)	Das (2015)
Case16-9-20	20 cm/s	Laakkonen *et al.* (2006) + Generalized PDF	Das (2015)
Case05-9-40	40 cm/s	Luo and Svendsen (1996)	Prince and Blanch (1990)
Case06-9-40	40 cm/s	Lehr *et al.* (2002)	Prince and Blanch (1990)
Case07-9-40	40 cm/s	Laakkonen *et al.* (2006)	Prince and Blanch (1990)
Case08-9-40	40 cm/s	Laakkonen *et al.* (2006) + Generalized PDF	Prince and Blanch (1990)
Case09-9-40	40 cm/s	Luo and Svendsen (1996)	Luo (1993)
Case10-9-40	40 cm/s	Lehr *et al.* (2002)	Luo (1993)
Case11-9-40	40 cm/s	Laakkonen *et al.* (2006)	Luo (1993)
Case12-9-40	40 cm/s	Laakkonen *et al.* (2006) + Generalized PDF	Luo (1993)
Case13-9-40	40 cm/s	Luo and Svendsen (1996)	Das (2015)
Case14-9-40	40 cm/s	Lehr *et al.* (2002)	Das (2015)
Case15-9-40	40 cm/s	Laakkonen *et al.* (2006)	Das (2015)
Case16-9-40	40 cm/s	Laakkonen *et al.* (2006) + Generalized PDF	Das (2015)

Table 6 Breakup and coalescence effect test settings

Turbulence Model:	Standard k-ε
Population Balance:	Discrete Method
Total Bin Number:	9 Bin
Drag Model:	Symmetric
Coalescence closure:	Prince and Blanch (1990) Luo (1993) Das (2015)
Breakup Closure:	Luo and Svendsen (1996) Lehr *et al.* (2002) Laakkonen *et al.* (2006) Laakkonen *et al.* (2006) + Generalized PDF
Inlet Boundary Condition:	Velocity-Inlet - Gas Superficial velocity: 20cm/s - Gas Superficial velocity: 40cm/s
Outlet Boundary Condition:	Pressure-Outlet - Atmospheric pressure
Wall Boundary Condition:	No-Slip

results were taken at the same height of the experimental data from Manjrekar and Dudukovic (2015) for validating purpose.

4.1 Effect of Drag Model Selection

The interfacial forces in bubbly flows still generates considerable debate among the researchers; however, it is a consensus that the drag force is the main interfacial force acting on the flow. Chen *et al.* (2005) and Silva *et al.*, (2014) affirmed that if drag is correctly modeled the other forces can be neglected in heterogeneous flow predictions.

The influence of the drag model on the prediction, in comparison with the experimental data of Manjrekar and Dudukovic (2015), is shown in Fig. 3. In all cases, the numerical results slightly overpredicted the axial velocity at the column center, but the Zhang and Vanderheyden (2002) model provided a better agreement with the experimental data. However, at the wall, this model underestimates the axial velocity, presenting a relative error around 79,96%, and the Symmetric model presents a better prediction with 17,05% of relative error. With regard to the gas holdup, this was overpredicted at the wall by all of the models and the Symmetric model presented a very good agreement at the column center with a relative error of 2.2%. Similar results were obtained by Soccol *et al.*, (2015) applying the Zhang and Vanderheyden (2002) and Schiller and Naumann (1935) models.

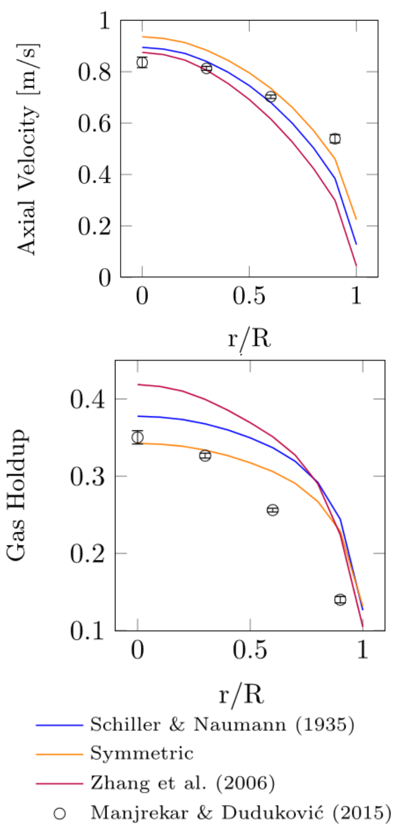

Fig. 3. Effect of drag models prediction.

It can be noted that the drag force has a strong influence on the flow dynamics. Based on the results obtained, the Symmetric model was applied in the subsequent simulations. The good agreement of the Symmetric model, with an average of 10,06% and 14,88% of relative error for axial velocity and gas holdup respectively, is due to the fact that for the experimental data used, small bubbles are dominant along the flow.

4.2 Effect of Breakage and Coalescence Models

For the effect of breakage and coalescence, a total of 24 simulations were conducted, applying 9 classes to solve the population balance equation and the Symmetric model for drag closure, at two different superficial velocities (20 and 40*cm/s*). Three coalescence models were evaluated Prince and Blanch (1990), Luo (1993) and Das (2015). With regard to the breakup models, those of Luo and Svendsen (1996), Lehr *et al.* (2002) and Laakkonen *et al.* (2006) were tested, the last one being associated with two different particle size distribution formulations: one proposed by the same authors and the other known as the generalized formulation, with three bubbles generated.

The coalescence models of Prince and Blanch (1990), Figs. 4 and 5, and Luo (1993), Figs. 6 and 7, produce similar results for both holdup and axial velocity, because they consider the same mechanism for the collision frequency term, which is based on the turbulence-induced theory, while for the coalescence efficiency the film drainage model was applied. For 20*cm/s* of gas superficial velocity, both cases presents good agreement with the experimental data at the column center for gas holdup, with relative errors around 7.2% and 6.2% respectively. While at the walls they overpredicted the experimental results. When combined with Lehr *et al.* (2002) the gas holdup at the center is also overpredicted. This phenomena is not observed at 40cm/s, probably due to the fact that this model considers that the breakup will occur if the inertial force of the bombarding eddy is greater than the interfacial force of the smallest daughter particle. Gas superficial velocity increase can be enhancing the eddy energy that hit the bubble, producing smaller bubbles, which decreases the gas holdup peak at the column center.

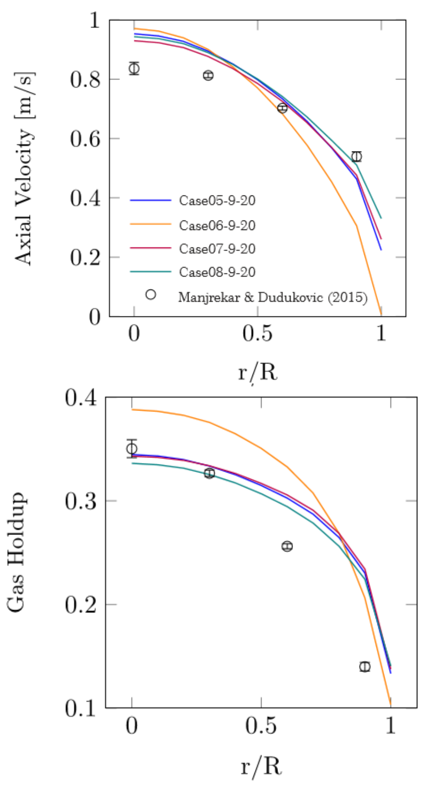

Fig. 4. Prince and Blanch (1990) coalescence model - gas superficial velocity of 20 *cm/s.*

For the gas axial velocity, at the smaller gas superficial velocity, both models (Prince and Blanch,

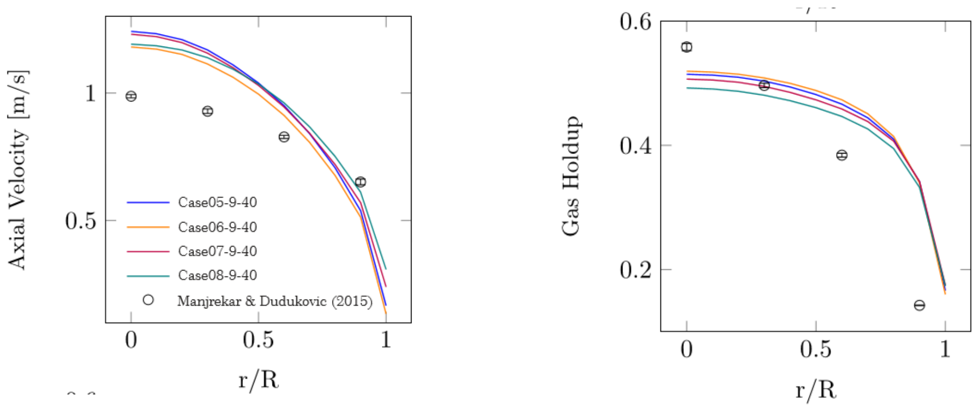

Fig. 5. **Prince and Blanch (1990) coalescence model - gas superficial velocity of 40 *cm/s*.**

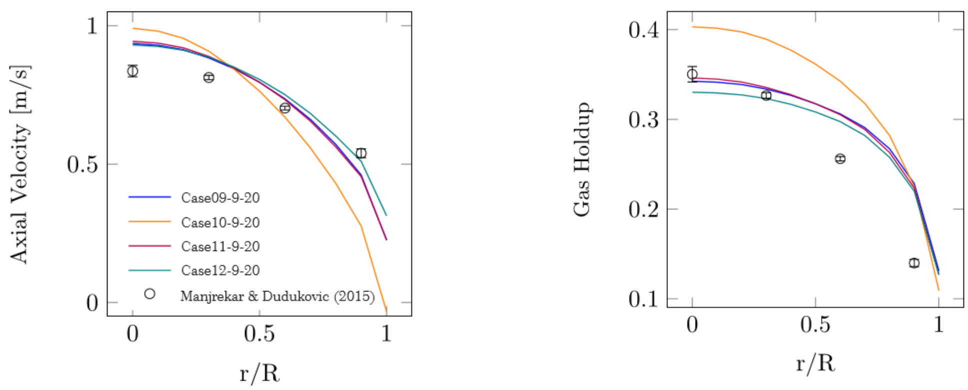

Fig. 6. **Luo and Svendsen (1996) coalescence model - gas superficial velocity of 20 *cm/s*.**

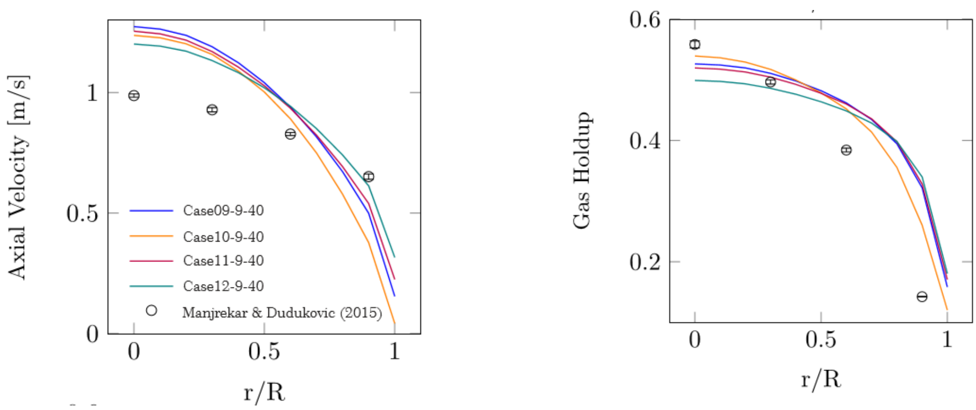

Fig. 7. **Luo and Svendsen (1996) coalescence model - gas superficial velocity of 40 *cm/s*.**

1990; Luo, 1993) shown better agreement near the column walls, excepting with the combination with Lehr *et al.* (2002) where the relative errors were of 76.32% when Prince and Blanch (1990) was applied, and of 95.11 with Luo (1993). For both cases, all models combinations were not able to reproduce the stepper profile of axial velocity at 40*cm/s*.

The Lehr *et al.* (2002) model considers that the breakup is dependent on a force balance between the interfacial surface and inertial forces of the hitting eddy, and only collisions with an eddy equal to or smaller than the size of the bubble result in breakup. Thus, the breakup is probably not achieved with this model, in contrast to the other models that consider a different breakup mechanism, which can lead to a predominance of coalescence, since bigger bubbles tend to migrate to the column center, making the gas axial velocity profile more parabolic and generating higher gas holdup. This finding can be corroborated by Fig. 10 where, for these cases, the bubble size distributions present higher values.

For a superficial gas velocity of 40*cm/s*, the dominance of coalescence is not observed, which could be due to the increase in the velocity making

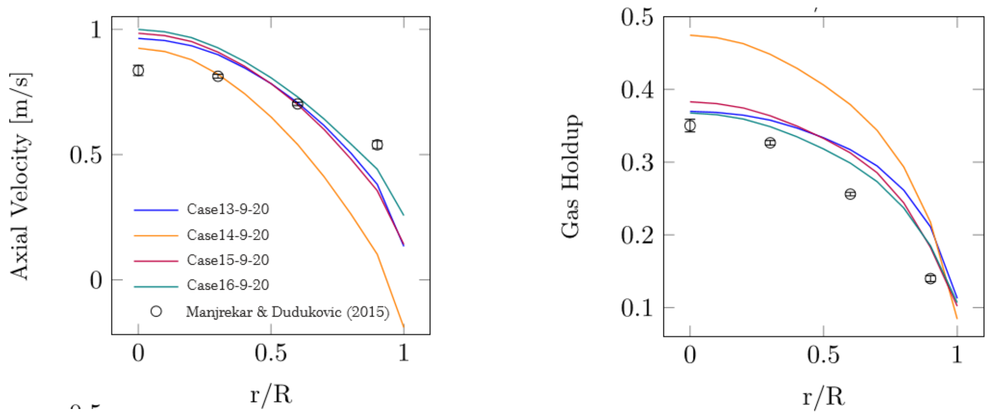

Fig. 8. Das (2015) **coalescence model - gas superficial velocity of 20** ***cm/s.***

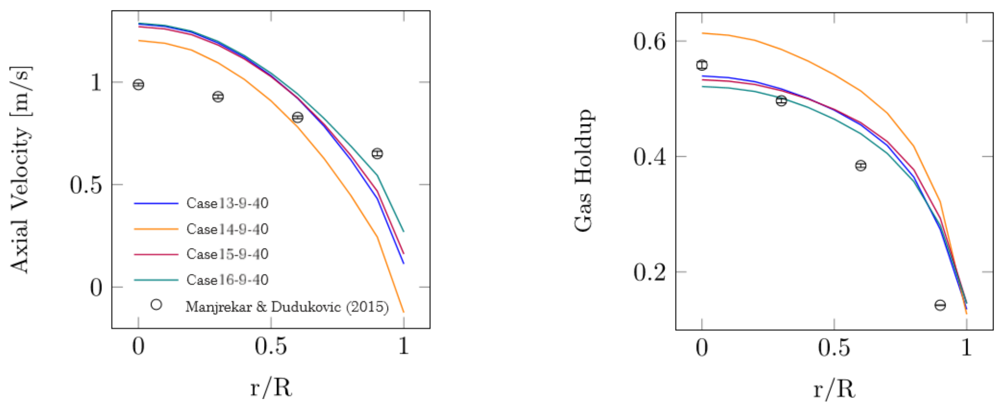

Fig. 9. Das (2015) **coalescence model - gas superficial velocity of 40** ***cm/s.***

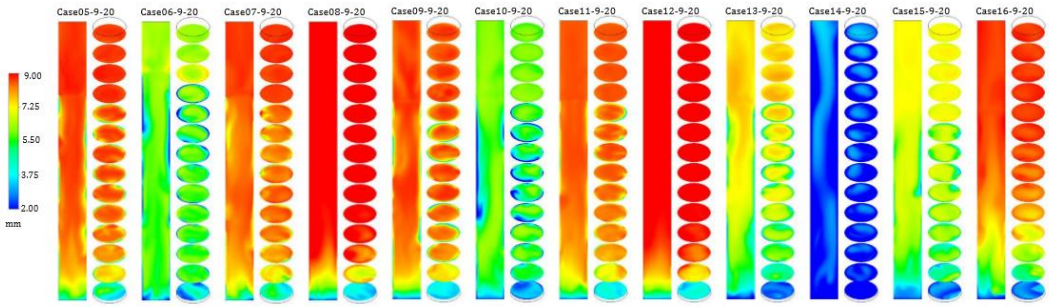

Fig. 10. Bubble size distribution - gas superficial velocity: 20 ***cm/s*** **at 120 seconds.**

the flow more unstable, generating smaller eddies that promote more bubble breakup.

When the coalescence model selected is that of Das (2015), Figs. 8 and 9, all models combinations result in similar profiles, with the exception of the Lehr *et al.* (2002) breakup model. In this case, an overprediction of the gas holdup was noted and a decrease in the gas axial velocity. Figures 10 and 11 show that for this model combination, a smaller bubble size diameter is achieved, which can be attributed to the dominance of breakup, resulting in small bubbles that rise more slowly than large ones, remaining for a longer time in the column and contributing to an increase in the gas holdup. When the Das (2015) coalescence model is applied, the same tendency with Prince and Blanch (1990) and Luo (1993) is observed. However, the relative errors with the experimental data are higher with this model, around 13% for axial velocity and 12% for gas holdup, for the best combination, with the break up model of Laakkonen *et al.* (2006) with generalized PDF, while with Prince and Blanch (1990) were about 7% and 13% and with Luo (1993) were 7% and 14%. Thus, we can conclude that the Das (2015) proposition needs improvement or perhaps a larger parametric study.

On maintaining the coalescence model and varying the breakup model, similar results were found using the models of Luo and Svendsen (1996), Laakkonen *et al.* (2006) and Laakkonen *et al.* (2006) with

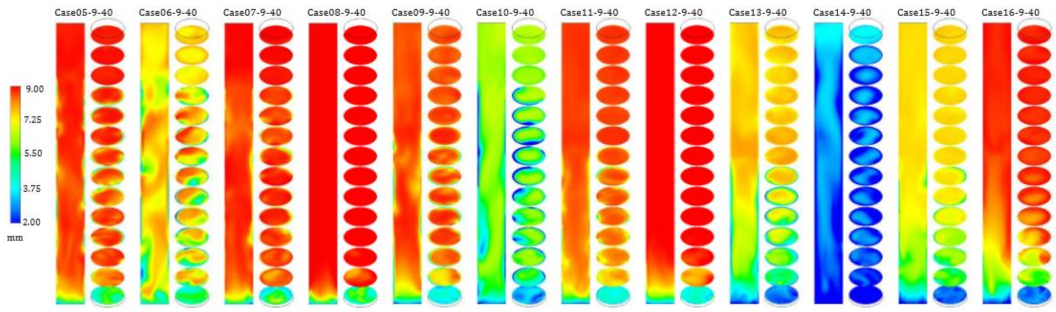

Fig. 11. Bubble size distribution - gas superficial velocity: 40 *cm/s* at 120 seconds.

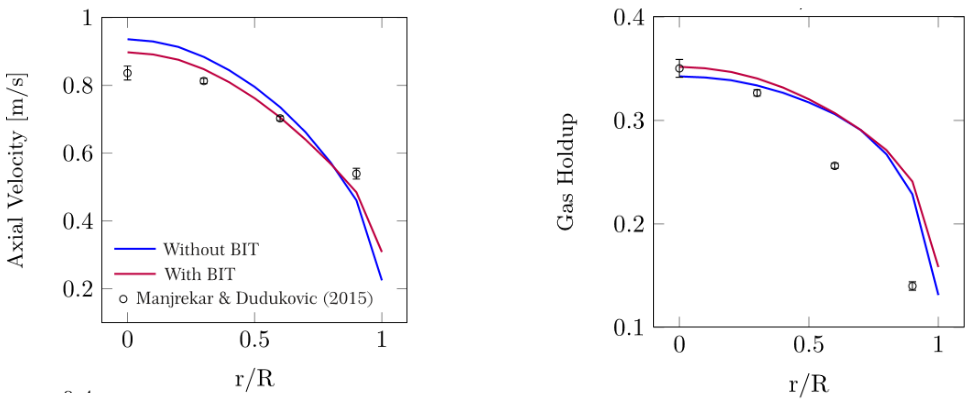

Fig. 12. Effect of bubble induced turbulence.

generalized PDF, and the last model presented better agreement with the experimental data of Manjrekar and Dudukovic (2015).

When the Lehr *et al.* (2002) breakage model was selected and the gas superficial velocity was 20*cm/s*, the simulation returned an overprediction of the gas holdup while the axial velocity was underestimated. As seen in Figs. 10 and 11, the cases where this model was applied showed a smaller mean bubble diameter compared to the other models. Laakkonen *et al.* (2007) also observed that the Lehr *et al.* (2002) model predicts a smaller bubble size distribution than that obtained experimentally. This behavior is probably related to the fact that in the Lehr *et al.* (2002) model the breakage is not dependent on the mother bubble size. In addition, the bigger the bubble size the higher the probability of collision will be with an eddy of the same or smaller size.

On the other hand, when the gas superficial velocity is equivalent to 40*cm/s* the differentiated behavior of the (Lehr, Millies, and Mewes, 2002) model is not as strong, and all of the breakage models show greater similarity with one another, mainly when the coalescence models of Luo (1993) or Prince and Blanch (1990) are used. In this case, the capillarity restraint probably plays a role. Wang *et al.* (2003) observed that as the bubble radius tends to zero, the interfacial force becomes stronger and the colliding eddy may not be able to provide sufficient dynamic pressure or inertial force to overcome the capillary pressure, even though sufficient energy is present (Liao and Lucas, 2009).

4.3 Effect of Bubble Induced Turbulence

The addition of a bubble induced turbulence model was also investigated. Case09-9-20

(Standard $k-\varepsilon$, Luo (1993) coalescence model, Luo and Svendsen (1996) breakup model, superficial gas velocity of 20*cm/s*) was compared with a simulation that employs the bubble induced turbulence of Sato and Sekoguchi (1975). In Fig. 12 the axial velocity of the gas phase and the gas holdup profiles are represented. In both cases, the BIT improves the numerical results at the column center, however, for gas holdup, even with its inclusion in the model, k-ε model overpredicts the gas holdup close to the wall Yamoah *et al.* (2015), Deju *et al.* (2013) The results show that the inclusion of the BIT model leads to an improvement on the validation against the experimental data, making the relative error of the axial velocity drop from around 10% to about 5.6%, as shown in Table 7.

5. CONCLUSION

Three-dimensional transient simulations were performed to verify the influence of the breakup and coalescence models on the prediction of heterogeneous bubbly flows.

For the population balance, a class method was employed, which demands an initial bubble size class, chosen according with experimental data.

The numerical investigations revealed that the correct choice of breakage and coalescence closures is crucial to the simulation success. In addition, from those evaluated, the breakup model had a greater influence on the flow prediction than the coalescence model.

Of the coalescence models analysed, those proposed by Prince and Blanch (1990) and Luo (1993) provided the most similar results, since they assume the same mechanisms, differing only in relation to the constants of the collision frequency term.

For breakup, the combination of the Laakkonen *et al.* (2006) model with the generalized PDF distribution and breakage generating three daughter bubbles provided good agreement with the experimental data, and this was the least demanding breakup closure in terms of computational time.

In the matter of drag closures, good agreement was observed for the modified Schiller and Naumann (1935) model, known as Symmetric model, probably due to the small bubble size predominance on the flow.

In this study, due to the high gas superficial velocities evaluated, the turbulence was set for both phases, employing the standard $k-\varepsilon$ approach. Results show good agreement with the experimental data. Besides, bubble induced turbulence was also included in the model, resulting in a better agreement at the column center for the gas axial velocity. However, at the walls, this approach overpredicts the experimental data.

Table 7 Relative Error - Effect of BIT

Case:	Without BIT		With BIT	
r/R	Axial Velocity	Gas Holdup	Axial Velocity	Gas Holdup
0	10.67	2.26	6.83	0.44
0.3	8.02	2.15	4.10	4.10
0.6	4.50	16.33	0.40	16.60
0.9	17.05	38.77	11.29	41.92
Average	10.06	14.88	5.66	15.77

ACKNOWLEDGMENTS

This study was financed in part by the Coordena¸cõo de Aperfeiçoamento de Pessoal de Nível Superior - Brasil (CAPES) - Finance Code 001.

REFERENCES

Alopaeus, V., J. Koskinen, K. I. Keskinen and J. Majander (2002). Simulation of the population balances for liquidliquid systems in a nonideal stirred tank. Part 2parameter fitting and the use of the multiblock model for dense dispersions. *Chemical Engineering Science* 57(10), 1815-1825.

Celik, I. B., U. Ghia, P. J. Roache, C. J. Freitas, H. Coleman and P. E. Raad (2008). Procedure for Estimation and Reporting of Uncertainty Due to Discretization in CFD Applications. *Journal of Fluids Engineering* 130(7), 78001.

Chen, P., J. Sanyal and M. Duduković (2005). Numerical simulation of bubble columns flows: effect of different breakup and coalescence closures. *Chemical Engineering Science* 60(4), 1085-1101.

Chesters, A. K. (1991). The Modeling of Coalescence Processes in Fluid-Liquid Dispersions. *Transactions of the Institution of Chemical Engineers* 69, 259-270.

Das, S. (2015). Development of a coalescence model due to turbulence for the population balance equation. *Chemical Engineering Science* 137, 22-30.

Deju, L., S. C. P. Cheung, G. H. Yeoh, F. Qi and J. Tu (2015). Comparative Analysis of Coalescence and Breakage Kernels in Vertical Gas-Liquid Flow. *The Canadian Journal of Chemical Engineering* 93(7), 1295-1310.

Deju, L., S. Cheung, G. Yeoh and J. Tu (2013). Capturing coalescence and break-up processes in vertical gas-liquid flows: Assessment of population balance methods. *Applied Mathematical Modelling* 37(18-19), 8557-8577.

Diemer, R. and J. Olson (2002). A moment methodology for coagulation and breakage problems: Part 2: moment models and distribution reconstruction. *Chemical Engineering Science* 57(12), 2211-2228.

Guan, X., Y. Gao, Z. Tian, L. Wang, Y. Cheng and X. Li (2015). Hydrodynamics in bubble columns with pin-fin tube internals. *Chemical Engineering Research and Design* 102, 196-206.

Hinze, J. O. (1959). *Turbulence*. Nova York: McGraw-Hill.

Howarth, W. (1964). Coalescence of drops in a turbulent flow field. *Chemical Engineering Science* 19(1), 33-38.

Hulburt, H. and S. Katz (1964). Some problems in particle technology. *Chemical Engineering Science* 19(8), 555-574.

Jakobsen, H. A., H. Lindborg and C. A. Dorao (2005). Modeling of Bubble Column Reactors: Progress and Limitations. *Industrial & Engineering Chemistry Research* 44(14), 5107-5151.

Joshi, J. B., K. Nandakumar, G. M. Evans, V. K. Pareek, M. M. Gumulya, M. J. Sathe and M. A. Khanwale (2017). Bubble generated turbulence and direct numerical simulations. *Chemical Engineering Science* 157, 26-75.

Kantarci, N., F. Borak and K. O. Ulgen (2005). Bubble column reactors. *Process Biochemistry* 40(7), 2263-2283.

Laakkonen, M., P. Moilanen, V. Alopaeus and J. Aittamaa (2007). Modelling local bubble size distributions in agitated vessels. *Chemical Engineering Science* 62(3), 721-740.

Laakkonen, M., V. Alopaeus and J. Aittamaa (2006). Validation of bubble breakage, coalescence and mass transfer models for gas-liquid dispersion in agitated vessel. *Chemical Engineering Science* 61(1), 218-228.

Launder, B. E. and D. B. Spalding (1972). Lectures in Mathematical Models of Turbulence. Academic Press 1, 492.

Lehr, F., M. Millies and D. Mewes (2002). Bubble-Size distributions and flow fields in bubble columns. *AIChE Journal* 48(11), 2426-2443.

Lelouvetel, J., Tanaka T., Y. Sato and K. Hishida (2014). Transport mechanisms of the turbulent energy cascade in upward downward bubbly flows. *Journal of Fluid Mechanics* 741, 514-542.

Leonard, C., J. H. Ferrasse, O. Boutin, S. Lefevre and A. Viand (2015). Bubble column reactors for high pressures and high temperatures operation. *Chemical Engineering Research and Design* 100, 391-421.

Liao, Y. (2014). *Development and Validation of Models for Bubble Coalescence and Breakup*. Ph.d., Dresden University of Technology.

Liao, Y. and D. Lucas (2009). A literature review of theoretical models for drop and bubble breakup in turbulent *dispersions. Chemical Engineering Science* 64(15), 3389-3406.

Liao, Y. and D. Lucas (2010). A literature review on mechanisms and models for the coalescence process of fluid particles. *Chemical Engineering Science* 65(10), 2851-2864.

Liu, Y. and N. Dinh (2019). Validation and Uncertainty Quantification for Wall Boiling Closure Relations in Multiphase-CFD Solver. *Nuclear Science and Engineering* 193(1-2), 81-99.

Liu, Y. and O. Hinrichsen (2014). Study on CFD-PBM turbulence closures based on k-ε and Reynolds stress models for heterogeneous bubble column flows. *Computers & Fluids* 105, 91-100.

Liu, Y., C. Rollins, N. Dinh and H. Luo (2017). Sensitivity Analysis of Interfacial Momentum Closure Terms in Two Phase Flow and Boiling Simulations Using MCFD Solver. In Volume 2: Heat Transfer Equipment; Heat Transfer in Multiphase Systems; Heat Transfer Under Extreme Conditions; Nanoscale Transport Phenomena; Theory and Fundamental Research in Heat Transfer; *Thermophysical Properties; Transport Phenomena in Materials* Pr, V002T11A004. ASME.

Luo, H. A. (1993). *Coalescence, Breakup and Liquid Circulation in Bubble Column Reactors.* Phd thesis, University of Trondhein.

Luo, H. and H. F. Svendsen (1996). Theoretical model for drop and bubble breakup in turbulent dispersions. *AIChE Journal* 42(5), 1225-1233.

Ma, M., J. Lu and G. Tryggvason (2016). Using statistical learning to close two-fluid multiphase flow equations for bubbly flows in vertical channels. *International Journal of Multiphase Flow* 85, 336-347.

Ma, M., J. Lu, and G. Tryggvason (2015). Using statistical learning to close two-fluid multiphase flow equations for a simple bubbly system. *Physics of Fluids* 27(9), 092101.

Manjrekar, O. N. and M. P. Dudukovic (2015). Application of a 4-point optical probe to a Slurry Bubble Column Reactor. *Chemical Engineering Science* 131, 313-322.

Montoya, G., D. Lucas, E. Baglietto and Y. Liao (2016). A review on mechanisms and models for the churn-turbulent flow regime. *Chemical Engineering Science* 141, 86-103.

Narsimhan, G., J. Gupta and D. Ramkrishna (1979). A model for transitional breakage probability of droplets in agitated lean liquid-liquid dispersions. *Chemical Engineering Science* 34(2), 257-265.

Prince, M. J. and H. W. Blanch (1990). Bubble coalescence and break-up in air-sparged bubble columns. *AIChE Journal* 36(10), 1485-1499.

Risso, F. and J. Fabre (1998). Oscillations and breakup of a bubble immersed in a turbulent field. *Journal of Fluid Mechanics* 372, 323-355.

Rollbusch, P., M. Bothe, M. Becker, M. Ludwig, M. Grünewald, M. Schlüter and R. Franke (2015). Bubble columns operated under industrially relevant conditions-Current understanding of design parameters. *Chemical Engineering Science* 126, 660-678.

Rzehak, R. and E. Krepper (2015). Bubbly flows with fixed polydispersity: Validation of a baseline closure model. *Nuclear Engineering and Design* 287, 108-118.

Sajjadi, B., A. A. A. Raman, R. S. S. R. E. Shah and S. Ibrahim (2013). Review on Applicable breakup/coalescence models in turbulent liquid-liquid flows. *Reviews in Chemical Engineering* 29(3), 131-158.

Sannáes, B. H. and D. Schanke (2004). Resolving flow details in slurry bubble columns used for Fischer-Tropsch synthesis using computational fluid dynamics. In X. Bao and Y. Xu (Eds.), Studies in Surface Science and Catalysis (147 ed.), Volume 147, Dalian, China, pp. 265–270. Elsevier B.V.

Sathe, M., J. Joshi and G. Evans (2013). Characterization of turbulence in rectangular bubble column. *Chemical Engineering Science* 100, 52-68.

Sato, Y. and K. Sekoguchi (1975). Liquid velocity distribution in two-phase bubble flow.

International Journal Multiphase Flow 2(1), 79–95.

Schiller, L. and A. Naumann (1935). A drag coefficient correlation. *Vereins Dtsch. Ingenieure* 77, 318-320.

Sharaf, S., M. Zednikova, M. C. Ruzicka and B. J. Azzopardi (2016). Global and local hydrodynamics of bubble columns - Effect of gas distributor. *Chemical Engineering Journal* 288, 489-504.

Shinnar, R. and J. M. Church (1960). Statistical Theories of Turbulence in Predicting Particle Size in Agitated *Dispersions. Industrial & Engineering Chemistry* 52(3), 253-256.

Silva, M. K., M. A. D'Ávila and M. Mori (2012). Study of the interfacial forces and turbulence models in a bubble column. *Computers & Chemical Engineering* 44, 34-44.

Silva, M. K., V. T. Mochi, M. Mori and M. A. D'Ávila (2014). Experimental and 3D Computational Fluid Dynamics Simulation of a Cylindrical Bubble Column in the Heterogeneous Regime. *Industrial & Engineering Chemistry Research* 53(8), 3353-3362.

Soccol, R., A. C. Galliani Piscke, D. Noriler, I. C. Georg, and H. F. Meier (2015). Numerical analysis of the interphase forces in bubble columns using euler-euler modelling framework. *The Canadian Journal of Chemical Engineering* 93(11), 2055-2069.

Tryggvason, G., J. Lu and M. Ma (2018). Direct Numerical Simulations of Gas-Liquid Flows. In *Proceedings of the 10th International Symposium on Cavitation* (CAV2018). ASME Press.

Tryggvason, G., M. Ma and J. Lu (2016). DNSAssisted Modeling of Bubbly Flows in Vertical Channels. *Nuclear Science and Engineering* 184(3), 312-320.

Wang, Q. and W. Yao (2016). Computation and validation of the interphase force models for bubbly flow. *International Journal of Heat and Mass Transfer* 98, 799-813.

Wang, T. (2011). Simulation of bubble column reactors using CFD coupled with a population balance model. *Frontiers of Chemical Science and Engineering* 5(2), 162-172.

Wang, T. and J. Wang (2007). Numerical simulations of gas-liquid mass transfer in bubble columns with a CFD-PBM coupled model. *Chemical Engineering Science* 62(24), 7107-7118.

Wang, T., J. Wang and Y. Jin (2003). A novel theoretical breakup kernel function for bubbles/droplets in a turbulent flow. *Chemical Engineering Science* 58(20), 4629-4637.

Wörner, M. (2003). *A Compact Introduction to the Numerical Modeling of Multiphase Flows*. Technical report, Institut für Reaktor-sicherheit, Karlsruhe.

Xu, L., B. Yuan, H. Ni and C. Chen (2013). Numerical Simulation of Bubble Column Flows in Churn-Turbulent Regime: Comparison of Bubble Size Models. *Industrial & Engineering Chemistry Research* 52(20), 6794-6802.

Xue, J., M. Al-Dahhan, M. Dudukovic and R. Mudde (2008). Four-point optical probe for measurement of bubble dynamics: Validation of the technique. *Flow Measurement and Instrumentation* 19(5), 293-300.

Yamoah, S., R. Martínez-Cuenca, G. Monrós, S. Chiva and R. Macián-Juan (2015). Numerical investigation of models for drag, lift, wall lubrication and turbulent dispersion forces for the simulation of gas-liquid two-phase flow. *Chemical Engineering Research and Design* 98, 17-35.

Zhang, D. and W. Vanderheyden (2002). The effects of mesoscale structures on the disperse two-phase flows and their closures for dilute suspensions. *International Journal of Multi-phase Flows* 28, 805–822.